Extended range ultra-wideband millimeter-wave channel sounder with over-the-air calibration

Extended Range Ultra-Wideband Millimeter-Wave Channel Sounder with Over-The-Air Calibration

R. Schulpen, D. Konstantinou, S. Rommel, U. Johannsen, I. Tafur Monroy, A.B. Smolders
Department of Electrical Engineering, Eindhoven University of Technology, Eindhoven, The Netherlands
r.schulpen@tue.nl

***Abstract*—In this paper, an ultra-wideband millimeter-wave channel sounder is introduced. The channel sounder, consisting of a Vector Network Analyzer and 1 km of fiber, can perform high resolution channel sounding over long distances. A wired response calibration is compared to an over-the-air calibration. It is shown that the over-the-air calibration of the channel sounder increases the dynamic range in the power-delay-profile by 14 dB compared to the wired response calibration.**

***Index Terms*—Channel sounder, propagation, millimeter-wave, ultra-wideband, calibration.**

I. Introduction

An almost eightfold growth in the total mobile traffic data is expected by 2023 [1]. This increase in mobile data usage can be accommodated by using the large bandwidths available in the millimeter-wave band [2], [3]. The potential use of very high data rates in micro- and pico-cell scenarios requires more detailed knowledge of the channel than is needed for cellular communication below 6 GHz. Ultra-wideband (UWB) channel sounding measurements are needed for the accurate characterization of the wireless millimeter-wave channel.

There are various types of channel sounders, which can be divided into time and frequency domain methods. Popular time domain millimeter-wave channel sounders are the sliding correlator [4]–[6] and the wideband correlator [7], [8]. The wideband correlator has a shorter measurement time than the sliding correlator at the cost of a more expensive analog-to-digital converter, enabling characterization of time-variant channels. No cable connection is required between the transmitter and receiver of these channel sounders when high stability clocks are used.

The most popular frequency domain channel sounder is the Vector Network Analyzer (VNA) [9], [10], probably because of its omnipresence in radio-frequency (RF) laboratories. Advantages are its large bandwidth capability and tight synchronization. Its disadvantages are a long sweep time, limiting the VNA to time-invariant channel measurements, and the need for a wired connection between the transmitter and receiver. This wired connection limits the VNA in spatial measurement range, especially at millimeter-wave frequencies, where the cable losses are large compared to lower frequencies. This can be partly overcome by using additional amplifiers [11]. Another method to extend the range of the VNA is to use a low-loss optical fiber instead of a long coaxial cable. This has already been demonstrated at frequencies below 6 GHz [12] and at millimeter-wave frequencies, where intermediate frequency (IF) over fiber is used in combination with electrical up- and down-conversion [13].

In this paper, an UWB millimeter-wave channel sounder using a VNA in combination with millimeter-wave RF over 1 km of fiber is introduced, employing high bandwidth optical components for direct RF-over-fiber range extension. The frequency range of interest is 24.25-29.5 GHz, which covers both the n257 (26.5-29.5 GHz) and n258 (24.25-27.5 GHz) bands proposed by the 3rd Generation Partnership Project (3GPP) [14].

The use of fiber optics and a large bandwidth poses some challenges on the calibration of the channel sounder. The use of fiber optics eliminates the possibility to do a full 2-port calibration of the channel sounder, because the fiber optic setup does not provide a reverse path for RF signals. The large bandwidth, resulting in a high temporal resolution, makes the power delay profile (PDP) more vulnerable to spurious paths from double reflections inside the channel sounder. In this paper, an over-the-air (OTA) calibration is proposed as alternative to the conventional wired response calibration, which is often used in channel sounding. It is shown that the OTA calibration improves the dynamic range in the PDP by 14 dB for the extended range channel sounder.

This paper is organized as follows. In Section II, the channel sounder architecture is discussed. The wired and OTA calibration of the channel sounder are discussed in Section III. The performance of these calibration methods is assessed in Section IV. Finally, this paper is concluded in Section V.

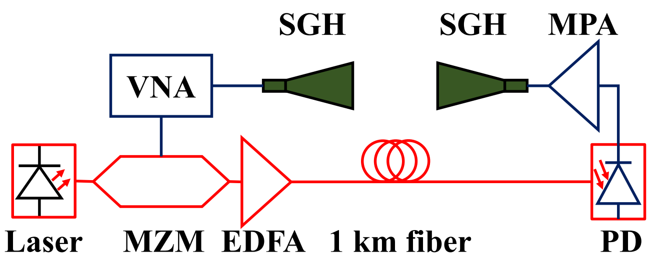

Fig. 1: Block diagram of the channel sounder with optical range extension.

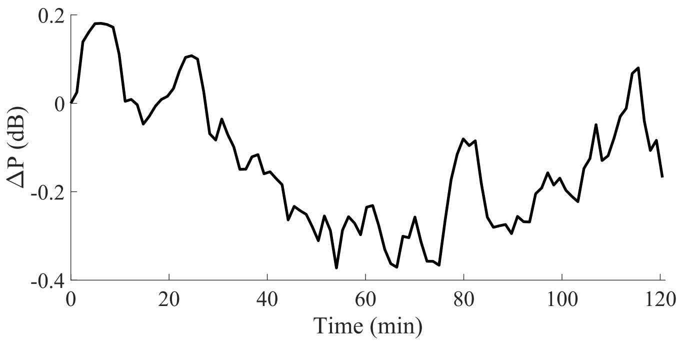

Fig. 2: Power variation of wired response measurement over time.

II. Channel Sounder Architecture

A block diagram of the channel sounder is depicted in Fig. 1. A VNA is used as synchronized RF transmitter and receiver. The transmitted signal is modulated onto an optical carrier by a Mach-Zehnder modulator (MZM). An erbium-doped fiber amplifier (EDFA) amplifies the signal before it is transmitted over a 1 km single-mode fiber (SMF). The optical power loss in this fiber is 0.2 dB/km. The optical signal is converted back to the electrical domain by a photodiode (PD). A medium-power amplifier (MPA) with 30 dB gain is used to compensate for the conversion losses. Standard gain horn (SGH) antennas with a gain of 18 dBi and a 3 dB beamwidth of 15° are used at the wireless interface.

32001 equally spaced frequency points between 24.25 GHz and 29.5 GHz are measured with the VNA, resulting in a temporal resolution of 0.19 ns, a spatial resolution of 5.7 cm, a maximum excess delay of 6.1 µs and an unambiguous free space range of 1.8 km. An IF bandwidth of 1 kHz and no averaging are used at the VNA, resulting in a maximum measurable path loss of 150 dB.

III. Channel Sounder Calibration

A calibration is required in order to extract the wireless channel from the measurement data, which also includes the response of the channel sounder itself. A full 2-port calibration of the complete channel sounder is not possible, because the optical setup does not provide a reverse path for the RF signals and the MPA requires a load. Alternative calibration methods are a wired frequency response calibration and an OTA calibration. These alternative methods should be combined with a full 2-port calibration of the VNA itself to correct for systematic errors inside the VNA. Thus all calibrations discussed in this paper were preceded by a full 2-port calibration of the VNA including the cables connected to it.

The response of the channel sounder should be stable before it is calibrated. Fig. 2 shows the variation in power over time of the wired response taken 90 min after the system was started. The maximum variation in power over two hours is 0.6 dB. This variation is caused by temperature changes, which lead to a change in bias point of the MZM and thus its effective transfer function. Using a thermoelectric controller (TEC) at the MZM would greatly reduce this variation. However, a TEC was not available during the measurements presented in this paper.

The wired and OTA calibrations are discussed in the next sections. These calibration methods are applied both to the complete channel sounder and to the VNA as reference system.

A. *Wired Calibration*

Fig. 3a depicts the wired calibration setup of the VNA. The full 2-port calibration, including a thru calibration with a calibration standard is all that is required for the wired calibration of the VNA. If done correctly, this calibration method fully de-embeds the measurement system excluding the antennas. If the antennas are not considered part of the

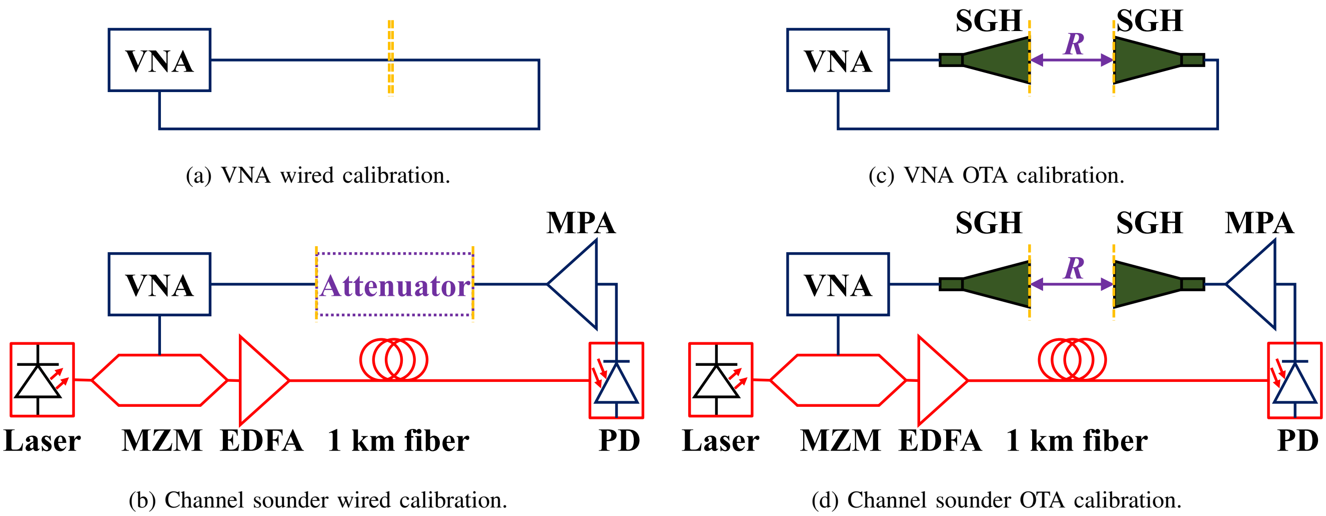

Fig. 3: Block diagrams of the different calibration setups for wired and OTA calibrations with and without the optical range extension.

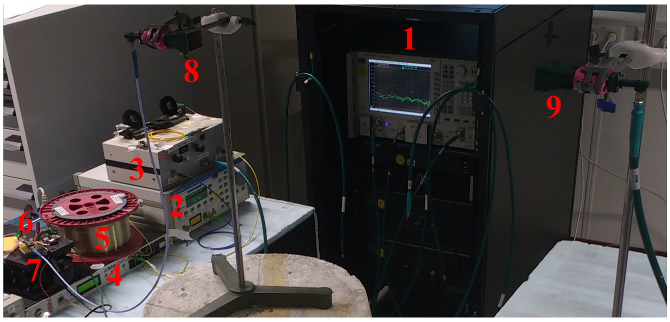

Fig. 4: OTA calibration setup of the channel sounder including the VNA (1), Laser (2), MZM (3), EDFA (4), 1 km fiber (5), PD (6), MPA (7), transmit SGH (8) and receive SGH (9).

channel, then double reflections inside the antennas can cause spurious paths.

A schematic overview of the wired calibration of the channel sounder is shown in Fig. 3b. An attenuator (of which a full S-parameter set is premeasured) is used to make the connection between the transmitter and receiver. The first step in this calibration is to obtain a full S-parameter set of the channel sounder plus attenuator. Then the attenuator is fully de-embedded by using the full S-parameter matrices of the attenuator and the channel sounder plus attenuator. The S_{21}-parameter of the de-embedded S-parameter set is the response of the wired system and hence dividing a measured S_{21}-parameter by this response results in a wired response calibration. In case of this wired response calibration, spurious paths can appear in measurement results due to a difference in match at the reference plane of the calibration between the cable that is connected to the MPA and the attenuator or antenna. The antennas are not included in this calibration method.

B. OTA Calibration

The OTA calibration is proposed here as alternative to the wired response calibration. The transmit and receive antennas are placed in a free space or anechoic environment pointing towards each other with their broadside directions aligned. This calibration includes the broadside response of the antennas and typically does not require the addition of an attenuator, because the path loss often adds sufficient attenuation. Reflections between the antennas or from the environment can introduce errors in this calibration method however. Also, misalignment of the antennas and separation distance errors can introduce additional errors. Paths that are not established via the broadside directions of the antennas are underestimated with this calibration method. Rotating the antennas and using digital signal processing (DSP) can correct for this.

Block diagrams for the OTA calibration of the VNA and channel sounder setups are depicted in Fig. 3c and Fig. 3d, respectively. A picture of the OTA calibration of the channel sounder is given in Fig. 4. This environment is not anechoic or completely free space, but is regarded as sufficiently free space for the calibration method comparison.

A reference distance R between the apertures of the antennas has to be chosen for the OTA calibration. For both the VNA and channel sounder, the S_{21}-parameter should be measured for this reference distance. This S_{21}-parameter contains the response of the measurement setup, the broadside response of the antennas, and the path loss and propagation delay of the wireless reference channel, where the assumption

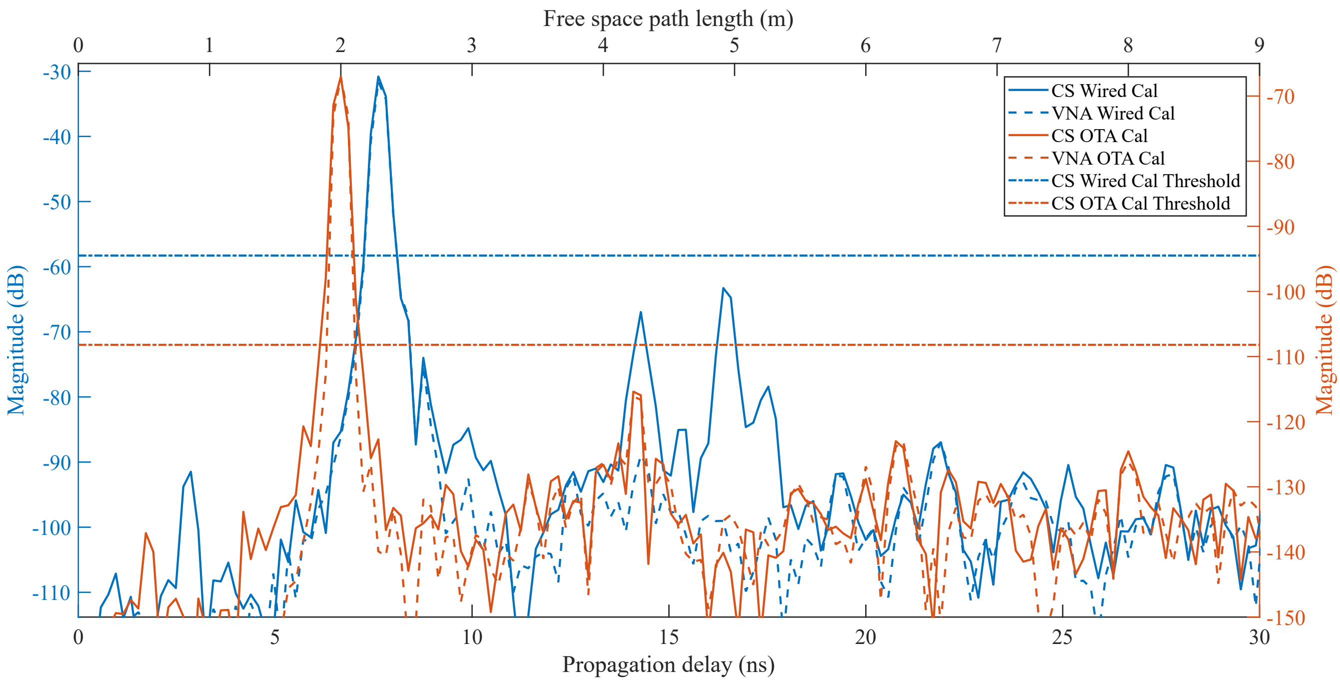

Fig. 5: Performance of the wired and OTA calibration methods for 2 m LOS measurements of the channel sounder and VNA.

is made that the path loss is equal to the free space path loss (FSPL). This assumption is valid if reflections from the environment (and a double reflection between the antennas) are sufficiently small. The path loss and propagation delay should be de-embedded from the reference. The FSPL as function of frequency can be calculated as

$$\mathrm{FSPL}(f) = \left(\frac{4\pi R f}{c}\right)^2 \tag{1}$$

where f is the frequency and c the speed of light. The calculated values in (1) can become inaccurate for small distances R, because the FSPL equation is valid in the far-field for the distance between the phase centers of the antennas, which is larger than the distance between the apertures in case of the SGH antennas. The calculated FSPL can be corrected by using the formulas in [15]. The FSPL correction for the SGH antennas is ranging from 0.07 dB to 0.12 dB over the frequency range 24.25-29.5 GHz for a distance R of 1 m. The propagation delay can be compensated for in the frequency domain by applying a frequency dependent phase shift. This phase shift can be calculated as

$$\phi(f) = \frac{2\pi R f}{c}. \tag{2}$$

A measurement can be calibrated by dividing by the S_{21}-parameter of the reference measurement, which is compensated by the corrected FSPL and propagation delay. This calibration method fully de-embeds the measurement system up to the apertures of the antennas. Spurious paths can occur due to bounces between the antennas and reflections from the environment in the reference measurement.

IV. Calibration Methods Performance

The performance of the wired and OTA calibration methods is assessed using a 2 m LOS measurement for both the VNA and channel sounder. The first 30 ns of the corresponding PDPs are depicted in Fig. 5. A Hanning window is applied to all measurements.

A. Wired Calibration

The main peaks in case of the wired calibration arrive at 7.6 ns for both the VNA and channel sounder measurements, which correspond to a free space path length of 2.3 m. This is the 2 m distance between the apertures of the antennas plus the length of the antennas. The magnitudes of these main peaks are -31.6 dB and -30.8 dB for the VNA and channel sounder measurements, respectively, which include the FSPL and the antenna gain. The large difference in magnitude can be explained by the conversion of the setup between the VNA and channel sounder measurements, which increased the variation in temperature and thus the variation in measured power. The largest spurious path of the channel sounder occurs after 16.4 ns with a magnitude of -63.3 dB and a delay of 8.8 ns with respect to the main peak. This delay corresponds to a bounce between the MPA and transmit antenna over the 1 m cable connecting both (taking into account the velocity factor of the cable). The spurious path at 14.3 ns is probably a reflection in the same cable due to a bend. The peaks at 8.8, 15.3 and 17.5 ns are bounces between the aperture of the antenna and respectively, the input of the antenna itself, the bend in the cable and the MPA. A threshold in the PDP is defined 5 dB above the largest spurious peak, which results in a dynamic range of 27 dB after a wired calibration of the channel sounder.

B. OTA Calibration

A similar analysis can be performed for the OTA calibration. A reference distance of 1 m is used. The main peaks have a delay of 6.7 ns for both the VNA and channel sounder measurements, which corresponds to the 2 m distance between the antenna apertures. The measured path loss is -67.1 dB for the VNA measurement and -67.0 dB for the channel sounder measurement. The -67.1 dB measured by the VNA is equal to the theoretical FSPL at the center frequency of 26.9 GHz. The largest spurious peak of the OTA calibration that is visible in Fig. 5 arrives at 14.1 ns with a magnitude of -115.4 dB. This is the bounce between the transmit and receive antenna in the 1 m reference measurement. Another spurious peak (not shown in Fig. 5), with a magnitude of -113.3 dB occurs after 114.5 ns, which corresponds to a path length of 34.4 m. This peak is probably due to a reflection from the environment. This spurious path limits the dynamic range of the PDP to 41 dB for the OTA calibrated channel sounder, including a margin of 5 dB. This is an improvement of 14 dB compared to the wired calibration. Measuring the wireless reference over a longer distance in a better anechoic or free space environment has the potential of further increasing the dynamic range in case of the OTA calibration.

V. Conclusion

An UWB millimeter-wave channel sounder is presented in this paper. A high performance VNA is combined with a 1 km low loss optical extension, resulting in a channel sounder that is capable of performing high resolution measurements over long distances. It is shown that an OTA calibration is more accurate than a wired response calibration in case of this channel sounder, resulting in a 14 dB larger dynamic range in the PDP.

Acknowledgment

This work is part of the Flagship Telecom collaboration between KPN and the Eindhoven University of Technology and partially funded by the 5G STEP FWD and blueSPACE projects with funding from the European Union's Horizon 2020 research and innovation programme under grant agreement numbers 722429 and 762055, respectively.

References

[1] P. Cerwall, A. Lundvall, P. Jonsson, S. Carson, and R. Möller, "Ericsson mobility report," 2018.

[2] Z. Pi and F. Khan, "An introduction to millimeter-wave mobile broadband systems," *IEEE communications magazine*, vol. 49, no. 6, 2011.

[3] T. S. Rappaport, S. Sun, R. Mayzus, H. Zhao, Y. Azar, K. Wang, G. N. Wong, J. K. Schulz, M. Samimi, and F. Gutierrez Jr, "Millimeter wave mobile communications for 5G cellular: It will work!" *IEEE access*, vol. 1, no. 1, pp. 335–349, 2013.

[4] T. S. Rappaport, E. Ben-Dor, J. Murdock, and Y. Qiao, "38 GHz and 60 GHz angle-dependent propagation for cellular & peer-to-peer wireless communications." in *Proc. IEEE Int. Conf. Commun.*, 2012, pp. 4568–4573.

[5] H.-K. Kwon, M.-D. Kim, and Y.-j. Chong, "Implementation and performance evaluation of mmWave channel sounding system," in *IEEE International Symposium on Antennas and Propagation & USNC/URSI National Radio Science Meeting*. IEEE, 2015, pp. 1011–1012.

[6] G. R. MacCartney and T. S. Rappaport, "A flexible millimeter-wave channel sounder with absolute timing," *IEEE Journal on Selected Areas in Communications*, vol. 35, no. 6, pp. 1402–1418, 2017.

[7] P. B. Papazian, C. Gentile, K. A. Remley, J. Senic, and N. Golmie, "A radio channel sounder for mobile millimeter-wave communications: System implementation and measurement assessment," *IEEE Transactions on Microwave Theory and Techniques*, vol. 64, no. 9, pp. 2924–2932, 2016.

[8] Z. Wen, H. Kong, Q. Wang, S. Li, X. Zhao, M. Wang, and S. Sun, "mmWave channel sounder based on COTS instruments for 5G and indoor channel measurement," in *Wireless Communications and Networking Conference (WCNC)*. IEEE, 2016, pp. 1–7.

[9] P. F. M. Smulders and A. G. Wagemans, "Wideband indoor radio propagation measurements at 58 GHz," *Electronics letters*, vol. 28, no. 13, pp. 1270–1272, 1992.

[10] X. Wu, Y. Zhang, C.-X. Wang, G. Goussetis, M. M. Alwakeel *et al.*, "28 GHz indoor channel measurements and modelling in laboratory environment using directional antennas," in *9th European Conference on Antennas and Propagation (EuCAP)*. IEEE, 2015, pp. 1–5.

[11] M. Lei, J. Zhang, T. Lei, and D. Du, "28-GHz indoor channel measurements and analysis of propagation characteristics," in *IEEE 25th Annual International Symposium on Personal, Indoor, and Mobile Radio Communication (PIMRC)*. IEEE, 2014, pp. 208–212.

[12] J. Medbo, M. Riback, H. Asplund, and J. Berg, "MIMO channel characteristics in a small macrocell measured at 5.25 GHz and 200 MHz bandwidth," in *IEEE 62nd Vehicular Technology Conference*, vol. 1. IEEE, 2005, pp. 372–376.

[13] K. Haneda, S. L. H. Nguyen, J. Järveläinen, and J. Putkonen, "Estimating the omni-directional pathloss from directional channel sounding," in *10th European Conference on Antennas and Propagation (EuCAP)*. IEEE, 2016, pp. 1–5.

[14] 3GPP, "TR 38.815 V15.0.0 (2018-06)."

[15] T. S. Chu and R. A. Semplak, "Gain of electromagnetic horns," *The Bell System Technical Journal*, vol. 44, no. 3, pp. 527–537, 1965.